© 2018 IJSRSET | Volume 4 | Issue 1 | Print ISSN: 2395-1990 | Online ISSN : 2394-4099
Themed Section : Engineering and Technology

Advances In Voronoi Hybrid Finite Element Elements

Yi Xiao

Research School of Engineering, Australian National University, Acton, ACT 2601, Australia

ABSTRACT

This paper presents an overview on developments of Voronoi hybrid finite element method (FEM). Recent developments on Special n-sided Voronoi fiber/matrix elements as well as Voronoi polygonal hybrid FEM with boundary integrals are described. Formulations for all cases are derived by means of modified variational functional and fundamental solutions. Generation of elemental stiffness equations from the modified variational principle is also discussed. Finally, a brief summary of the approach and potential research topics is provided.
Keywords: Finite Element Method, Fundamental Solution, Voronoi elements.

I. INTRODUCTION

Applications of various numerical methods have been attractive by many researchers in recent years [1-4]. It should be mentioned that analytical solutions which are available only for a few problems with simple geometries and boundary conditions [5-18]. Therefore, development of efficient numerical methods is vital for solving engineering problems [19-25]. A new method, the so-called hybrid Trefftz FEM (or T-Trefftz method) has been developed recently [26, 27]. Unlike in the conventional FEM, the T-Trefftz method couples the advantages of conventional FEM [28-31] and BEM [32-34]. In contrast to the standard FEM, the T-Trefftz method is based on a hybrid method which includes the use of an independent auxiliary inter-element frame field defined on each element boundary and an independent internal field chosen so as to a prior satisfy the homogeneous governing differential equations by means of a suitable truncated T-complete function set of homogeneous solutions. Since 1970s, T-Trefftz model has been considerably improved and has now become a highly efficient computational tool for the solution of complex boundary value problems. It has been applied to potential problems [35-38], two-dimensional elastics [39, 40], elastoplasticity [41, 42], fracture mechanics [43-45], micromechanics analysis [46, 47], problem with holes [48, 49], heat conduction [50-52], thin plate bending [53-56], thick or moderately thick plates [57-61], three-dimensional problems [62], piezoelectric materials [63-67], and contact problems [68-70].

On the other hand, the hybrid FEM based on the fundamental solution (F-Trefftz method for short) was initiated in 2008 [27, 71] and has now become a very popular and powerful computational methods in mechanical engineering. The F-Trefftz method is significantly different from the T-Trefftz method discussed above. In this method, a linear combination of the fundamental solution at different points is used to approximate the field variable within the element. The independent frame field defined along the element boundary and the newly developed variational functional are employed to guarantee the inter-element continuity, generate the final stiffness equation and establish linkage between the boundary frame field and internal field in the element. This review will focus on the F-Trefftz finite element method.

The F-Trefftz finite element method, newly developed recently [27, 71], has gradually become popular in the field of mechanical and physical engineering since it is initiated in 2008 [27, 72, 73]. It has been applied to potential problems [37, 74-76], plane elasticity [40, 77, 78], composites [79-83], piezoelectric materials [84-86], three-dimensional problems [87], functionally graded materials [88-90], bioheat transfer problems [91-97], thermal elastic problems [98], hole problems [99, 100], heat conduction problems [71, 101], micromechanics problems [46, 47], and anisotropic elastic problems [102-104].

Following this introduction, the present review consists of 3 sections. Special n-sided Voronoi fiber/matrix elements for clustering thermal effect is presented in Section 2. It describes in detail the method of deriving element stiffness equations. Section 3 focuses on the essentials of Voronoi polygonal hybrid finite elements with boundary integrals. Finally, a brief summary of the developments of the Voronoi element methods is provided.

II. SPECIAL N-SIDED VORONOI FIBER/MATRIX ELEMENTS

2.1 Micromechanical model of clustered composite

For a periodic cement-based composite containing clustered hemp fibers, the representative unit cell is the smallest repeated microstructure of the composite that can be isolated from the composite to estimate the composite's effective properties. It is assumed that the unit cell has same thermal properties and fiber volume contents as the composite under consideration.

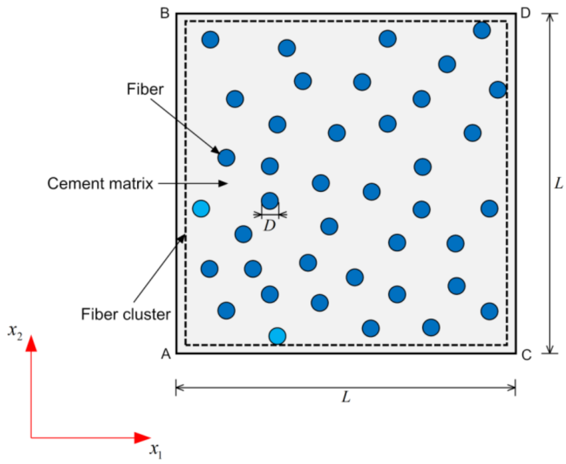

Figure 1. Schematic representation of regularly and randomly clustered fibers within the cement matrix

Figure 1 shows a representative unit cell containing clustered hemp fibers. In Fig. 1, L denotes the cell length, D is the diameter of the hemp fiber, and x_1 and x_2 are the global coordinate axial directions. Under the assumptions that (1) all material constituents are isotropic and homogeneous, and (2) the hemp fiber and the cement matrix are perfectly bonded, the steady-state local temperature fields in the matrix and the fiber, denoted by T_m and T_f, should satisfy the two-dimensional heat conduction governing equations respectively, given by

$$\frac{\partial^2 T_m}{\partial x_1^2}+\frac{\partial^2 T_m}{\partial x_2^2}=0, \quad \frac{\partial^2 T_f}{\partial x_1^2}+\frac{\partial^2 T_f}{\partial x_2^2}=0 \qquad (1)$$

and the continuous conditions at the interface between the hemp fiber and the matrix

$$T_m = T_f$$
$$k_m \frac{\partial T_m}{\partial n} = k_f \frac{\partial T_f}{\partial n} \qquad (2)$$

where n is the unit direction normal to the fiber/matrix interface.

According to Fourier's law of heat transfer in isotropic media, we have the following relationship of the temperature variable T and the heat flux component q_i:

$$q_i = -k\frac{\partial T}{\partial x_i} \qquad (i=1,2) \qquad (2)$$

from which the effective thermal conductivity k_e of the homogenized composite can be determined by

$$k_e = \frac{\bar{q}_i}{\bar{\varepsilon}_i} \tag{3}$$

where $\bar{q}_i$ stands for the area-averaged heat flux component along the *i*-direction and $\bar{\varepsilon}_i$ the temperature gradient component along the *i*-direction. For example, for the applied temperature boundary conditions below

$$\begin{aligned} T_m &= T_0 && \text{on edge AB} \\ T_m &= T_1 && \text{on edge CD} \\ k_m \frac{\partial T_m}{\partial n} &= 0 && \text{on edges AC and BD} \end{aligned} \tag{4}$$

the effective thermal conductivity k_e of the composite can be calculated by the 1-directional average heat flux component $\bar{q}_1$ on the surface CD and the 1-directional temperature gradient component $\bar{\varepsilon}_1$ respectively given by

$$\bar{q}_1 = \frac{1}{L}\int_{AB} q_1(x_1, x_2)\mathrm{d}x_2 \tag{5}$$

$$\bar{\varepsilon}_1 = \frac{(T_1 - T_2)}{L} \tag{6}$$

2.2 Formulation of special n-sided Voronoi fiber/matrix element

The representative unit cell with the specified temperature conditions along the outer boundary of the cell is solved by a fundamental-solution-based hybrid finite element formulation with special n-sided Voronoi fiber/matrix elements. To efficiently treat regularly and randomly clustered distributions of hemp fibers in the unit cell and obtain a mesh with relatively high quality, the centroidal Voronoi tessellation technique is employed such that the generators for the Voronoi tessellation and the centroids of the Voronoi regions coincide. The centroidal Voronoi tessellation technique can be viewed as an optimal partition corresponding to an optimal distribution of generators. Fig. 2 displays a typical n-sided Voronoi fiber/matrix element division for the composite cell including hemp fiber and cement material constituents. As an example, in Fig. 2, the centroidal Voronoi elements are iteratively generated by the matlab source code using 25 random points in the cell and the fibers are located at the centroids of the Voronoi elements.

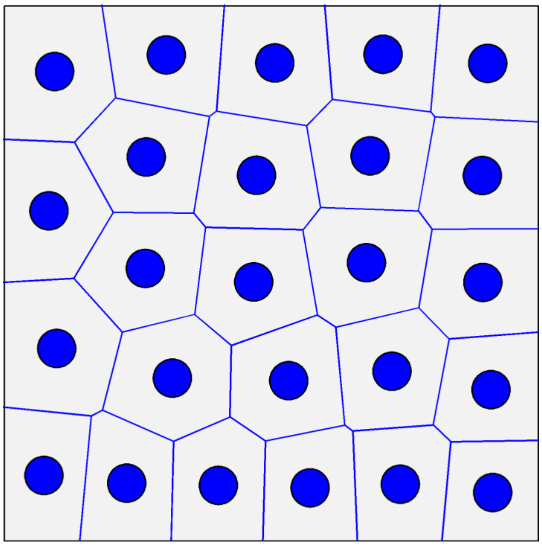

Figure 2. Schematic diagram of n-sided Voronoi fiber/matrix elements for the case of a random cluster

For a typical *n*-sided Voronoi fiber/matrix element *e*, with element domain Ω_e and element boundary Γ_e, the assumed fields include:

(a) Non-conforming interior temperature field

$$T(\mathbf{x}) = \sum_{j=1}^{m} G(\mathbf{x}, \mathbf{x}_{sj}) c_{ej} = \mathbf{N}_e \mathbf{c}_e \qquad \mathbf{x} \in \Omega_e \tag{7}$$

(b) Auxiliary conforming frame temperature field

$$\tilde{T}(\mathbf{x}) = \tilde{\mathbf{N}}_e \mathbf{d}_e \qquad \mathbf{x} \in \Gamma_e \tag{8}$$

where G is the fundamental solutions satisfying equilibrium and continuity within the element, $\mathbf{x}(x_1, x_2)$ and $\mathbf{x}_{sj}(x_{1j}^s, x_{2j}^s)$ are the field point and source point, respectively, $\mathbf{N}_e$ is a row vector of fundamental solutions, $\mathbf{c}_e$ is a column vector of the unknown coefficient c_{ej}, $\tilde{\mathbf{N}}_e$ represents a row vector of the conventional interpolating shape functions, and $\mathbf{d}_e$ is a column vector of the nodal degree of freedom of the element.

Subsequently, the heat flux field in the element can be derived by means of Fourier's law

$$q_i(\mathbf{x}) = -k\frac{\partial T(\mathbf{x})}{\partial x_i} = \mathbf{T}_{ei}\mathbf{c}_e \qquad \mathbf{x} \in \Omega_e \tag{9}$$

with

$$\mathbf{T}_{ei} = -k\frac{\partial \mathbf{N}_e}{\partial x_i} \tag{10}$$

Furthermore, the outward normal heat flux q_n derived from the interior field T_e can be expressed as

$$q_n = q_1 n_1 + q_2 n_2 = \mathbf{Q}_e \mathbf{c}_e \tag{11}$$

with

$$\mathbf{Q}_e = \mathbf{T}_{e1} n_1 + \mathbf{T}_{e2} n_2 \tag{12}$$

and n_i $(i=1,2)$ are components of the outward unit normal to the element boundary.

To link the two independent fields above, the element variational functional is of the form

$$\Pi_{me} = -\frac{1}{2}\int_{\Omega_e} k\left(\frac{\partial^2 T}{\partial x_1^2} + \frac{\partial^2 T}{\partial x_2^2}\right)\mathrm{d}\Omega - \int_{\Gamma_{eq}} \bar{q}\tilde{T}\mathrm{d}\Gamma + \int_{\Gamma_e} q_n\left(\tilde{T} - T\right)\mathrm{d}\Gamma \tag{13}$$

in which Γ_{eq} is the element heat flux boundary, and $\bar{q}$ is the specified normal heat flux.

Application of the divergence theorem to the functional (13) yields

$$\Pi_{me} = -\frac{1}{2}\int_{\Gamma_e} q_n T\mathrm{d}\Gamma - \int_{\Gamma_{qe}} \bar{q}\tilde{T}\mathrm{d}\Gamma + \int_{\Gamma_e} q_n \tilde{T}\mathrm{d}\Gamma \tag{14}$$

Then, substituting Eqs. (7) and (8) into the functional (14) yields

$$\Pi_{me} = -\frac{1}{2}\mathbf{c}_e{}^{\mathrm{T}}\mathbf{H}_e\mathbf{c}_e - \mathbf{d}_e{}^{\mathrm{T}}\mathbf{g}_e + \mathbf{c}_e{}^{\mathrm{T}}\mathbf{G}_e\mathbf{d}_e \tag{15}$$

in which

$$\mathbf{H}_e = \int_{\Gamma_e} \mathbf{Q}_e^{\mathrm{T}}\mathbf{N}_e\mathrm{d}\Gamma,\ \mathbf{G}_e = \int_{\Gamma_e} \mathbf{Q}_e^{\mathrm{T}}\tilde{\mathbf{N}}_e\mathrm{d}\Gamma,\ \mathbf{g}_e = \int_{\Gamma_{eq}} \tilde{\mathbf{N}}_e^{\mathrm{T}}\bar{q}\mathrm{d}\Gamma$$

Minimization of the functional Π_{me} with respect to $\mathbf{c}_e$ and $\mathbf{d}_e$, respectively, yields

$$\frac{\partial \Pi_{me}}{\partial \mathbf{c}_e{}^{\mathrm{T}}} = -\mathbf{H}_e\mathbf{c}_e + \mathbf{G}_e\mathbf{d}_e = \mathbf{0},\quad \frac{\partial \Pi_e}{\partial \mathbf{d}_e{}^{\mathrm{T}}} = \mathbf{G}_e{}^{\mathrm{T}}\mathbf{c}_e - \mathbf{g}_e = \mathbf{0} \tag{16}$$

from which the optional relationship between $\mathbf{c}_e$ and $\mathbf{d}_e$ for enforcing inter-element continuity on the common element boundary

$$\mathbf{c}_e = \mathbf{H}_e{}^{-1}\mathbf{G}_e\mathbf{d}_e \tag{17}$$

and the element stiffness equation including the element stiffness matrix $\mathbf{K}_e$ and the equivalent nodal force vector $\mathbf{g}_e$

$$\mathbf{K}_e\mathbf{d}_e = \mathbf{g}_e \tag{18}$$

can be obtained. In Eq. (18), $\mathbf{K}_e = \mathbf{G}_e{}^{\mathrm{T}}\mathbf{H}_e{}^{-1}\mathbf{G}_e$ is symmetric. Evidently, evaluation of Ke involves inversion of the symmetric square He matrix, and it's advantageous to use a minimum number of source points outside the element for improving inversion efficiency. In contrast, accuracy is generally improved if a large number of source points is used. In this study, the number of source points is chosen to be same as that of element nodes to balance the requirements of efficiency and accuracy. Certainly, the rank sufficiency condition in the hybrid finite element method is also satisfied. In addition, different to the Voronoi cell finite element method, the present method is a type of hybrid displacement finite element method and all integrals involved are along element boundary only. However, the present method requires the fundamental solutions of the related problem, which are not available for some physical problems.

The following two-component heterogeneous fundamental solutions satisfying the equilibrium and continuity of fiber and matrix domains can be written as

$$G(z, z_{sj}) = -\frac{1}{2\pi k_m}\left\{\begin{aligned}&\mathrm{Re}\left[\ln(z - z_{sj})\right]\\&+\frac{k_m - k_f}{k_m + k_f}\mathrm{Re}\left[\ln(\frac{R^2}{z} - \bar{z}_{sj})\right]\end{aligned}\right\} \quad \text{for } z \in \Omega_m$$

$$G(z, z_{sj}) = -\frac{1}{(k_m + k_f)\pi}\mathrm{Re}\left[\ln(z - z_{sj})\right] \quad \text{for } z \in \Omega_f \tag{19}$$

where $z = x_1 + ix_2$ and $z_{sj} = x_{1j}^s + ix_{2j}^s$ are the complex coordinates of the field point and the source point, respectively, R is the radius of fiber inclusion, and $i = \sqrt{-1}$ is the imaginary unit. Ω_m and Ω_f are respectively the cement matrix domain and the hemp fiber domain. In particular, if $k_m = k_f = k$, Eq. (19) reduces to

$$G(z, z_{sj}) = -\frac{1}{2k\pi}\mathrm{Re}\left[\ln(z - z_{sj})\right] \tag{20}$$

which corresponds to the heat transfer caused by a point heat source in an isotropic homogeneous medium.

III. YORONOI POLYGONAL HYBRID FINITE ELEMENTS

3.1 Governing Equations for Plane Elasticity

For simplicity, our attention in this study is restricted to the classic linear isotropic elasticity in two dimensions, which have been solved by various numerical methods, i.e. FEM, BEM and meshless methods. As indicated in Fig. 1, a two-dimensional (2D) static linear isotropic elasticity domain Ω is bounded by the boundary $\Gamma=\Gamma_u \cup \Gamma_t$, $\Gamma_u \cap \Gamma_t = 0$. Γ_u and Γ_t are displacement and traction boundaries, respectively. Referred to the Cartesian coordinate system (x_1,x_2), the static equilibrium equation for the dashed linear elastic element around an arbitrary point $\mathbf{x}\equiv(x_1,x_2)$ (see Fig. 1) in the absence of body force is given in matrix form by

$$\mathbf{L}^{\mathrm{T}}\boldsymbol{\sigma}=0 \tag{22}$$

where $\boldsymbol{\sigma}=\{\sigma_{11},\sigma_{22},\sigma_{12}\}^{\mathrm{T}}$ is the stress vector, and $\mathbf{L}$ is the strain-displacement operator matrix

$$\mathbf{L}^{\mathrm{T}}=\begin{bmatrix} \dfrac{\partial}{\partial x_1} & 0 & \dfrac{\partial}{\partial x_2} \\ 0 & \dfrac{\partial}{\partial x_2} & \dfrac{\partial}{\partial x_1} \end{bmatrix} \tag{23}$$

The strain vector $\boldsymbol{\varepsilon}=\{\varepsilon_{11},\varepsilon_{22},\gamma_{12}\}^{\mathrm{T}}$ is defined by the kinematic relation as

$$\boldsymbol{\varepsilon}=\mathbf{L}\mathbf{u} \tag{24}$$

where $\mathbf{u}=\{u_1,u_2\}^{\mathrm{T}}$ is the displacement vector.

For the case of linear elastic solid body, the stress vector is related to the strain vector by the Hooke's law in matrix form

$$\boldsymbol{\sigma}=\mathbf{D}\boldsymbol{\varepsilon} \tag{25}$$

where $\mathbf{D}$ is the constitutive matrix and has the form

$$\mathbf{D}=\begin{bmatrix} \dfrac{E}{1-\nu^2} & \dfrac{\nu E}{1-\nu^2} & 0 \\ \dfrac{\nu E}{1-\nu^2} & \dfrac{E}{1-\nu^2} & 0 \\ 0 & 0 & \dfrac{E}{2(1+\nu)} \end{bmatrix} \tag{26}$$

for plane stress cases.

Besides, the following displacement and traction boundary conditions prescribed on the displacement boundary Γ_u and the traction boundary Γ_t

$$\begin{aligned} \mathbf{u}&=\bar{\mathbf{u}} \qquad \text{on } \Gamma_u \\ \mathbf{t}&=\bar{\mathbf{t}} \qquad \text{on } \Gamma_t \end{aligned} \tag{27}$$

should be augmented to form a complete solving system. In Eq. (27), $\bar{\mathbf{u}}$ and $\bar{\mathbf{t}}$ are respectively the specified displacement and traction constraints. According to the equilibrium of the dashed triangle shown in Fig. 3, the traction vector $\mathbf{t}=\{t_1,\ t_2\}^{\mathrm{T}}$ is expressed by

$$\mathbf{t}=\mathbf{A}\boldsymbol{\sigma} \tag{28}$$

where

$$\mathbf{A}=\begin{bmatrix} n_1 & 0 & n_2 \\ 0 & n_2 & n_1 \end{bmatrix} \tag{29}$$

and n_i $(i=1,2)$ are the unit outward normal components.

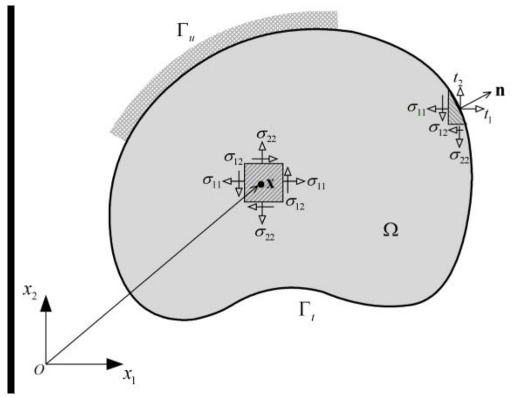

Figure 3. Schematic diagram for plane elastic problems

3.2 Conventional Finite Element Formulation

In this section, the finite element formulation with polygonal elements is reviewed for the purpose of comparison. In the conventional polygonal finite element theory, the displacement field at point with coordinate $\mathbf{x}\in\Omega_e$ is approximated for a typical polygonal finite element occupying the domain Ω_e by

$$\mathbf{u}=\sum_{i=1}^{n}\mathbf{U}_i\mathbf{d}_i=\mathbf{U}_e\mathbf{d}_e \tag{30}$$

where n is the total number of element nodes, $\mathbf{d}_i=\{u_{1i},\ u_{2i}\}^{\mathrm{T}}$ is the column vector of nodal degrees of freedom related to the *i*th node, $\mathbf{d}_e=\{\mathbf{d}_1^{\mathrm{T}} \quad \mathbf{d}_2^{\mathrm{T}} \quad \cdots \quad \mathbf{d}_n^{\mathrm{T}}\}^{\mathrm{T}}$

is the final nodal displacement vector of the element e, and $\mathbf{U}_e = [\mathbf{U}_1 \quad \mathbf{U}_2 \quad \cdots \quad \mathbf{U}_n]$ is the resulted finite element shape function matrix in which

$$\mathbf{U}_i = \begin{bmatrix} \phi_i & 0 \\ 0 & \phi_i \end{bmatrix} \tag{31}$$

is the element shape submatrix associated with the ith node and usually consists of two-dimensional element shape functions ϕ_i expressed in the following general form

$$\phi_i(\mathbf{x}) = \frac{w_i(\mathbf{x})}{\sum_{j=1}^{n} w_j(\mathbf{x})} \tag{32}$$

In Eq. (32), $w_i(\mathbf{x})$ are non-negative weight functions, which have differently defined for difference shape functions, i.e. Wachspress shape functions and Laplace shape functions.

Subsequently, the strain and stress fields defined by Eqs. (24) and (25) can be expressed in terms of nodal displacement vector $\mathbf{d}_e$, that is

$$\boldsymbol{\varepsilon} = \mathbf{L}\mathbf{u} = \mathbf{B}_e\mathbf{d}_e, \qquad \boldsymbol{\sigma} = \mathbf{D}\boldsymbol{\varepsilon} = \mathbf{D}\mathbf{B}_e\mathbf{d}_e \tag{33}$$

where

$$\mathbf{B}_e = \mathbf{L}\mathbf{U}_e = [\mathbf{L}\mathbf{U}_1 \quad \mathbf{L}\mathbf{U}_2 \quad \cdots \quad \mathbf{L}\mathbf{U}_n] \tag{34}$$

The final discrete equations can be formulated from the Galerkin weak or variational form

$$\int_{\Omega_e} \delta\boldsymbol{\varepsilon}^{\mathrm{T}}\boldsymbol{\sigma}\mathrm{d}\Omega - \int_{\Gamma_e^t} \delta\mathbf{u}^{\mathrm{T}}\bar{\mathbf{t}}\mathrm{d}\Gamma = 0 \tag{35}$$

where δ denotes the variational operator and $\Gamma_e^t = \Gamma_e \cap \Gamma_t$ is the element traction boundary.

Substituting the variational forms of the strain and displacement fields

$$\delta\mathbf{u} = \mathbf{U}_e\delta\mathbf{d}_e, \qquad \delta\boldsymbol{\varepsilon} = \mathbf{B}_e\delta\mathbf{d}_e \tag{36}$$

and Eq. (33) into Eq. (34) yields

$$\delta\mathbf{d}_e^{\mathrm{T}}\left(\int_{\Omega_e} \mathbf{B}_e^{\mathrm{T}}\mathbf{D}\mathbf{B}_e\mathrm{d}\Omega\right)\mathbf{d}_e - \delta\mathbf{d}_e^{\mathrm{T}}\left(\int_{\Gamma_e^t} \mathbf{U}_e^{\mathrm{T}}\bar{\mathbf{t}}\mathrm{d}\Gamma\right) = 0 \tag{37}$$

Invoking the arbitrariness of nodal variation $\delta\mathbf{d}_e$, we have

$$\mathbf{K}_e\mathbf{d}_e = \mathbf{f}_e \tag{38}$$

where

$$\mathbf{K}_e = \int_{\Omega_e} \mathbf{B}_e^{\mathrm{T}}\mathbf{D}\mathbf{B}_e\mathrm{d}\Omega, \qquad \mathbf{f}_e = \int_{\Gamma_e^t} \mathbf{U}_e^{\mathrm{T}}\bar{\mathbf{t}}\mathrm{d}\Gamma \tag{39}$$

It's obviously seen that the shape function and its derivatives are vital for the implementation of conventional finite element. The shape functions are defined for the entire element domain to locate and relate element nodes, so different shape functions bring different element matrices and different degrees of precision. For polygonal finite elements with large numbers of sides and nodes, it's very complicated to construct suitable weight functions so that the shape function satisfies all required properties, especially for polygonal elements with curved edges. This is the main reason that the topology of conventional finite element is usually restricted to triangle and quadrilateral for two-dimensional problems or tetrahedral and hexahedral for three-dimensional problems. Another key issue to be addressed is the evaluation of such domain integral in Eq. (39). So far, the numerical quadrature rule over arbitrary polygons has not yet reached a mature stage and the most popular approach is to partition the n-sided polygonal finite element (n>4) into n triangles by the centroid of the element and then use well-known quadrature rules on each triangle.

In this study, a different Voronoi polygonal hybrid finite element formulation based on the fundamental solutions of the two-dimensional linear elastic problem is presented below, which is fully independent of the construction of shape functions and the polygonal element domain integration.

3.3 Voronoi Polygonal Hybrid FE Formulation

The implementation of polygonal hybrid finite elements involves two important issues: (1) the geometrical description and mesh discretization of the enclosed computing domain with finite number of convex polygons and (2) element-level approximations of physical fields to accurately compute the design response.

For the first issue, the advanced Voronoi polygon meshing technique developed by Talischi et al [105] can be utilized to represent flexible mesh generation in arbitrary geometries. Mathematically, every common edge of a Voronoi polygonal cell is defined as being normal to the line connecting two neighboring seed points and has equivalent distance to them, so that Voronoi cells can easily possess more connected neighbors. Fig. 4(a) shows a Voronoi diagram and its Delaunay triangulation generated by the Voronoi tessellation technique and a particular polygonal Voronoi cell associated with seed point $\boldsymbol{p}$ is hatched as an example in the figure. As one of Voronoi cells, the centroidal Voronoi tessellation possessing the added attribution that the seed points are coincident with the cell centroids is employed in the study to produce high-quality convex polygonal discretization in the computing domain [106]. Moreover, to approximate the practical boundary of the domain during Voronoi meshing, the signed distance function is defined in Paulino's meshing scheme [107] to provide all essential information of the domain geometry so that one can flexibly construct the desired domain by algebraic expressions.

Secondly, after convex polygonal meshing is obtained, the fundamental solution based hybrid finite element technique is formulated here to convert the element domain integral into element boundary integrals and obtain the final solving system of equations. For a typical Voronoi polygonal hybrid finite element e occupying the domain Ω_e, as shown in Fig. 4(b), the linear combinations of displacement and stress fundamental solutions of the problem are respectively used as the approximation functions to model the intra-element displacement and stress fields within the element domain Ω_e

$$\begin{aligned} \mathbf{u}(\mathbf{x}) &= \sum_{k=1}^{m} \mathbf{N}_k(\mathbf{x})\mathbf{c}_k = \mathbf{N}_e(\mathbf{x})\mathbf{c}_e, \\ \boldsymbol{\sigma}(\mathbf{x}) &= \sum_{k=1}^{m} \mathbf{T}_k(\mathbf{x})\mathbf{c}_k = \mathbf{T}_e(\mathbf{x})\mathbf{c}_e, \quad \mathbf{x} \in \Omega_e \end{aligned} \tag{40}$$

with

$$\begin{aligned} \mathbf{N}_k &= \begin{bmatrix} u_{11}^*\left(\mathbf{x},\mathbf{x}_k^s\right) & u_{21}^*\left(\mathbf{x},\mathbf{x}_k^s\right) \\ u_{12}^*\left(\mathbf{x},\mathbf{x}_k^s\right) & u_{22}^*\left(\mathbf{x},\mathbf{x}_k^s\right) \end{bmatrix}, \\ \mathbf{T}_k &= \begin{bmatrix} \sigma_{111}^*\left(\mathbf{x},\mathbf{x}_k^s\right) & \sigma_{211}^*\left(\mathbf{x},\mathbf{x}_k^s\right) \\ \sigma_{122}^*\left(\mathbf{x},\mathbf{x}_k^s\right) & \sigma_{222}^*\left(\mathbf{x},\mathbf{x}_k^s\right) \\ \sigma_{112}^*\left(\mathbf{x},\mathbf{x}_k^s\right) & \sigma_{212}^*\left(\mathbf{x},\mathbf{x}_k^s\right) \end{bmatrix}, \quad \mathbf{c}_k = \{c_1^k, \quad c_2^k\}^{\mathrm{T}} \end{aligned} \tag{41}$$

where m is the number of source points $\mathbf{x}_k^s$ $(k = 1,\cdots,m)$ and in practice it can be chosen to be same as the number of nodes, as done in literature for general and special quadrilateral case. $\mathbf{c}_e = \{\mathbf{c}_1^{\mathrm{T}} \quad \mathbf{c}_2^{\mathrm{T}} \quad \cdots \quad \mathbf{c}_m^{\mathrm{T}}\}^{\mathrm{T}}$ is the unknown coefficient vector. $\mathbf{N}_e = [\mathbf{N}_1 \quad \mathbf{N}_2 \quad \cdots \quad \mathbf{N}_m]$ and $\mathbf{T}_e = [\mathbf{T}_1 \quad \mathbf{T}_2 \quad \cdots \quad \mathbf{T}_m]$ denote the matrices consisting of displacement fundamental solution $u_{li}^*(\mathbf{x},\mathbf{x}_k^s)$ $(l,i=1,2)$ and stress fundamental solution σ_{lij}^* $(l,i,j=1,2)$ at the field point $\mathbf{x}$ due to the unit force along the lth direction at the source points $\mathbf{x}_k^s$, respectively.

It's evident that the intra-element displacement and stress fields (40) can naturally satisfy the linear elastic governing equations (43) because of the physical definition of fundamental solutions, if a series of source points are placed outside the element as they are well done in the standard meshless method of fundamental solutions (MFS) [108].

However, the intra-element displacement field given by Eq. (40) is non-conforming across the inter-element boundary, as indicated by the shaded region in Fig. 4(b). To deal with such problem, the hybrid technique popularly used in the hybrid finite element method pioneered by Pian [109] is employed to introduce an auxiliary conforming displacement frame field which has similar form as that in the conventional FEM. Here, the independent displacement frame field defined along the element boundary Γ_e is written as

$$\tilde{\mathbf{u}}(\mathbf{x}) = \tilde{\mathbf{N}}_e(\mathbf{x})\mathbf{d}_e, \qquad \mathbf{x} \in \Gamma_e \tag{42}$$

where $\mathbf{d}_e$ is the nodal displacement vector same as that in Eq. (30), and $\tilde{\mathbf{N}}_e$ is the standard FE shape function matrix with one-dimensional shape functions for the two-dimensional problem considered in the paper. For example, if there are two nodes on a particular edge for the linear case, the shape function matrix over this edge can be written by

$$\tilde{\mathbf{N}}_e = \begin{bmatrix} \tilde{N}_1 & 0 & \tilde{N}_2 & 0 \\ 0 & \tilde{N}_1 & 0 & \tilde{N}_2 \end{bmatrix} \tag{43}$$

where $\tilde{N}_1 = (1-\xi)/2$, $\tilde{N}_2 = (1+\xi)/2$ are respectively the classic one-dimensional linear shape functions in terms of the natural coordinate ξ varying from -1 to 1, whose definition can be found in most of books on FEM.

To link these two independent fields, the double-variable weak variational form originally developed in literature [20, 27] for traditional eight-node quadrilateral elements is employed:

$$\Pi_{me} = \frac{1}{2}\int_{\Omega_e} \boldsymbol{\sigma}^{\mathrm{T}}\boldsymbol{\varepsilon}\mathrm{d}\Omega - \int_{\Gamma_e^t} \bar{\mathbf{t}}\tilde{\mathbf{u}}\mathrm{d}\Gamma + \int_{\Gamma_e} \mathbf{t}(\tilde{\mathbf{u}} - \mathbf{u})\mathrm{d}\Gamma \tag{44}$$

where $\Gamma_e^t = \Gamma_e \cap \Gamma_t$ and $\mathbf{t}$ is the traction field on the element boundary Γ_e and may be approximated by considering Eqs. (28) and (40) as

$$\mathbf{t} = \mathbf{A}\mathbf{T}_e\mathbf{c}_e = \mathbf{Q}_e\mathbf{c}_e \tag{45}$$

Due to the natural feature of the intra-element fields, Eq. (44) can be further simplified by applying the Gaussian theorem to the domain integral in it

$$\Pi_{me} = -\frac{1}{2}\int_{\Gamma_e} \mathbf{t}\mathbf{u}\mathrm{d}\Gamma - \int_{\Gamma_e^t} \bar{\mathbf{t}}\tilde{\mathbf{u}}\mathrm{d}\Gamma + \int_{\Gamma_e} \mathbf{t}\tilde{\mathbf{u}}\mathrm{d}\Gamma \tag{46}$$

Substituting the intra-element fields (40), (45) and the frame field (42) into the functional (46) yields

$$\Pi_{me} = -\frac{1}{2}\mathbf{c}_e^{\mathrm{T}}\mathbf{H}_e\mathbf{c}_e - \mathbf{d}_e^{\mathrm{T}}\mathbf{g}_e + \mathbf{c}_e^{\mathrm{T}}\mathbf{G}_e\mathbf{d}_e \tag{47}$$

where

$$\mathbf{H}_e = \int_{\Gamma_e} \mathbf{Q}_e^{\mathrm{T}}\mathbf{N}_e\mathrm{d}\Gamma,\ \ \mathbf{G}_e = \int_{\Gamma_e} \mathbf{Q}_e^{\mathrm{T}}\tilde{\mathbf{N}}_e\mathrm{d}\Gamma,\ \ \mathbf{g}_e = \int_{\Gamma_e^t} \tilde{\mathbf{N}}_e^{\mathrm{T}}\bar{\mathbf{t}}\mathrm{d}\Gamma \tag{48}$$

To enforce inter-element continuity on the common element boundary, the unknown vector $\mathbf{c}_e$ should be expressed in terms of nodal degree of freedom $\mathbf{d}_e$. The minimization of the functional Π_{me} in Eq. (47) with respect to $\mathbf{c}_e$ and $\mathbf{d}_e$, respectively, yields

$$\frac{\partial \Pi_{me}}{\partial \mathbf{c}_e^{\mathrm{T}}} = -\mathbf{H}_e\mathbf{c}_e + \mathbf{G}_e\mathbf{d}_e = \mathbf{0},\quad \frac{\partial \Pi_{me}}{\partial \mathbf{d}_e^{\mathrm{T}}} = \mathbf{G}_e^{\mathrm{T}}\mathbf{c}_e - \mathbf{g}_e = \mathbf{0} \tag{49}$$

from which we can obtain the element stiffness equation

$$\mathbf{K}_e\mathbf{d}_e = \mathbf{g}_e \tag{50}$$

and the optional relationship of $\mathbf{c}_e$ and $\mathbf{d}_e$

$$\mathbf{c}_e = \mathbf{H}_e^{-1}\mathbf{G}_e\mathbf{d}_e \tag{51}$$

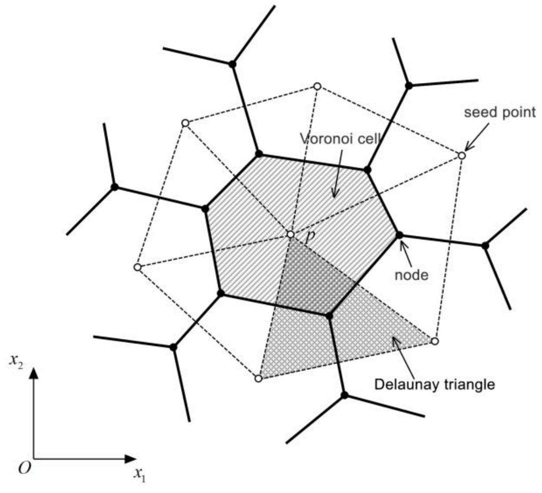

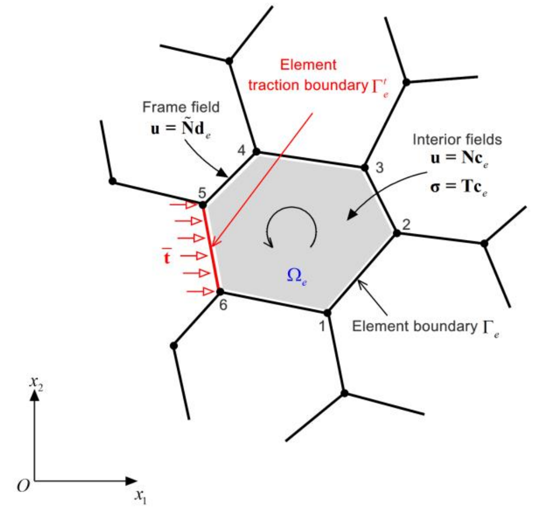

Figure 4. Illustration of Voronoi polygonal hybrid finite elements

where the element stiffness matrix $\mathbf{K}_e = \mathbf{G}_e^{\mathrm{T}}\mathbf{H}_e^{-1}\mathbf{G}_e$ only consists of numerical integrals of the symmetric matrix $\mathbf{H}_e$ and the matrix $\mathbf{G}_e$ over the element boundary Γ_e. In practice, they can be evaluated by the well-known one-dimensional Gaussian quadrature rule along the element sides of the polygon one by one, without any difficulty, as indicated in Reference [27], thus the present hybrid strategy is very suitable for constructing n-sided polygonal finite elements. Besides, we observe that the introduction of conforming frame displacement field permits the direct imposition of essential boundary conditions and the direct evaluation of effect of traction boundary conditions, as done in the classic FEM.

IV. CONCLUSIONS

On the basis of the preceding discussion, the following conclusions can be drawn. This review reports recent developments on the formulation of Voronoi hybrid FEM. It proved to be a powerful computational tool in modeling materials and structures with various mechanical properties. However, there are still many possible extensions and areas in need of further development in the future. Among those developments one could list the following:

1. Development of efficient Voronoi FE-BEM schemes for complex engineering structures containing heterogeneous materials and the related general-purpose computer codes with preprocessing and postprocessing capabilities.
2. Generation of various special-purpose elements to effectively handle singularities attributable to local geometrical or load effects (holes, cracks, inclusions, interface, corner and load singularities). The special-purpose functions warrant that excellent results are obtained at minimal computational cost and without local mesh refinement.
3. Development of Voronoi FE in conjunction with a topology optimization scheme to contribute to microstructure design.
4. Extension of Voronoi FEM to elastodynamics and fracture mechanics of FGMs.

V. REFERENCES

[1]. Y. Xiao, A. Abdollahi, Q.H. Qin, Quantitatively structuring a trabecular network using computational geometry techniques, Universal Journal of Engineering Science, 2(1) (2014) 30-37.

[2]. B.H. Zhao, C.Y. Qu, Q.H. Qin, Bone distribution simulation during damage-repair bone remodeling in human proximal femur, Advanced Materials Research, 634 (2013) 883-891.

[3]. K. Cai, Q.H. Qin, Z. Luo, A. Zhang, Robust topology optimisation of bi-modulus structures, Computer-Aided Design, 45(10) (2013) 1159-1169.

[4]. Q.S. Yang, Q.H. Qin, T. Liu, Interlayer stress in laminate beam of piezoelectric and elastic materials, Composite structures, 75(1) (2006) 587-592.

[5]. Q.H. Qin, Y.W. Mai, A closed crack tip model for interface cracks in thermopiezoelectric materials, International Journal of Solids and Structures, 36(16) (1999) 2463-2479.

[6]. S.W. Yu, Q.H. Qin, Damage analysis of thermopiezoelectric properties: Part II. Effective crack model, Theoretical and Applied Fracture Mechanics, 25(3) (1996) 279-288.

[7]. Q.H. Qin, 2D Green's functions of defective magnetoelectroelastic solids under thermal loading, Engineering Analysis with Boundary Elements, 29(6) (2005) 577-585.

[8]. Q.H. Qin, General solutions for thermopiezoelectrics with various holes under thermal loading, International Journal of Solids and Structures, 37(39) (2000) 5561-5578.

[9]. Q.H. Qin, Green's function and boundary elements of multifield materials, Elsevier, Oxford, 2007.

[10]. Q.H. Qin, Y.W. Mai, S.W. Yu, Some problems in plane thermopiezoelectric materials with holes, International Journal of Solids and Structures, 36(3) (1999) 427-439.

[11]. Q.H. Qin, Y.W. Mai, Crack growth prediction of an inclined crack in a half-plane thermopiezoelectric solid, Theoretical and Applied Fracture Mechanics, 26(3) (1997) 185-191.

[12]. Q.H. Qin, Fracture mechanics of piezoelectric materials, WIT Press, Southampton, 2001.

[13]. Q.H. Qin, S.W. Yu, An arbitrarily-oriented plane crack terminating at the interface between dissimilar piezoelectric materials, International Journal of Solids and Structures, 34(5) (1997) 581-590.

[14]. S.W. Yu, Q.H. Qin, Damage analysis of thermopiezoelectric properties: Part I—crack tip singularities, Theoretical and Applied Fracture Mechanics, 25(3) (1996) 263-277.

[15]. J.S. Wang, G.F. Wang, X.Q. Feng, Q.H. Qin, Surface effects on the superelasticity of nanohelices, Journal of Physics: Condensed Matter, 24(26) (2012) 265303.

[16]. J.S. Wang, X.Q. Feng, J. Xu, Q.H. Qin, S.W. Yu, Chirality transfer from molecular to morphological scales in quasi-one-dimensional nanomaterials: a continuum model, Journal of Computational and Theoretical Nanoscience, 8(7) (2011) 1278-1287.

[17]. J.-S. Wang, G.-F. Wang, X.-Q. Feng, Q.-H. Qin, Surface effects on the superelasticity of nanohelices, Journal of Physics: Condensed Matter, 24(26) (2012) 265303.

[18]. Y. Wang, Q.H. Qin, A theoretical study of bone remodelling under PEMF at cellular level, Computer Methods in Biomechanics and Biomedical Engineering, 15(8) (2012) 885-897.

[19]. H. Wang, Q.H. Qin, Y. Xiao, Special n-sided Voronoi fiber/matrix elements for clustering thermal effect in natural-hemp-fiber-filled cement composites, International Journal of Heat and Mass Transfer, 92 (2016) 228-235.

[20]. Q.H. Qin, The Trefftz finite and boundary element method, WIT Press, Southampton, 2000.

[21]. Q.H. Qin, Trefftz finite element method and its applications, Applied Mechanics Reviews, 58(5) (2005) 316-337.

[22]. H. Wang, Q.H. Qin, Y. Kang, A meshless model for transient heat conduction in functionally graded materials, Computational Mechanics, 38(1) (2006) 51-60.

[23]. N. Bavi, Q.H. Qin, B. Martinac, Finite element simulation of the gating mechanism of mechanosensitive ion channels, in: Fourth International Conference on Smart Materials and Nanotechnology in Engineering, International Society for Optics and Photonics, 2013, pp. 87931S-87931S-87937.

[24]. C. Liu, Y. Zhang, Q.H. Qin, R.B. Heslehurst, Numerical Modelling of Glass Fibre Metal Laminates Subjected to High Velocity Impact, in: Proceedings of the Composites Australia and CRC-ACS, 2013 Composites Conference (Edited by Rikard Heslehurst), Melbourne, 4-5 March 2013, 2013.

[25]. C.J. Liu, Y. Zhang, Q.H. Qin, R. Heslehurst, High velocity impact modelling of sandwich panels with aluminium foam core and aluminium sheet skins, in: Applied Mechanics and Materials, 2014, pp. 745-750.

[26]. Z.-J. Fu, Q.H. Qin, W. Chen, Hybrid-Trefftz finite element method for heat conduction in nonlinear functionally graded materials, Engineering Computations, 28(5) (2011) 578-599.

[27]. Q.H. Qin, H. Wang, Matlab and C programming for Trefftz finite element methods, New York: CRC Press, 2008.

[28]. Q.H. Qin, C.X. Mao, Coupled torsional-flexural vibration of shaft systems in mechanical engineering—I. Finite element model, Computers & Structures, 58(4) (1996) 835-843.

[29]. H.C. Martin, G.F. Carey, Introduction to finite element analysis: Theory and application, McGraw-Hill New York, 1973.

[30]. H. Wang, Y. Xiao, Q.H. Qin, 2D hierarchical heat transfer computational model of natural ber bundle reinforced composite, Scientia Iranica, Transactions B: Mechanical Engineering, 23(1) (2016) 268-276.

[31]. K.Z. Ding, Q.H. Qin, M. Cardew-Hall, A New Integration Algorithm for the Finite Element Analysis of Elastic-Plastic Problems, in: Proc. of 9th International Conference on Inspection, Appraisal, Repairs & Maintenance of Structures, Fuzhou, China, 20-21 October, CI-Premier PTY LTD, ISBN: 981-05-3548-1, 2005, pp. 209-216.

[32]. Q.H. Qin, Y.W. Mai, BEM for crack-hole problems in thermopiezoelectric materials, Engineering Fracture Mechanics, 69(5) (2002) 577-588.

[33]. Q.H. Qin, Y. Huang, BEM of postbuckling analysis of thin plates, Applied Mathematical Modelling, 14(10) (1990) 544-548.

[34]. Q.H. Qin, Nonlinear analysis of Reissner plates on an elastic foundation by the BEM, International journal of solids and structures, 30(22) (1993) 3101-3111.

[35]. W. Chen, Z.-J. Fu, Q.-H. Qin, Boundary particle method with high-order Trefftz functions, Computers, Materials & Continua (CMC), 13(3) (2010) 201-217.

[36]. H. Wang, Q.H. Qin, D. Arounsavat, Application of hybrid Trefftz finite element method to non-linear problems of minimal surface, International Journal for Numerical Methods in Engineering, 69(6) (2007) 1262-1277.

[37]. H. Wang, Q.-H. Qin, X.-P. Liang, Solving the nonlinear Poisson-type problems with F-Trefftz hybrid finite element model, Engineering Analysis with Boundary Elements, 36(1) (2012) 39-46.
[38]. L.-L. Cao, Q.H. Qin, N. Zhao, A new RBF-Trefftz meshless method for partial differential equations, IOP Conference Series: Materials Science and Engineering, 10 (2010) 012217.
[39]. Q.H. Qin, Dual variational formulation for Trefftz finite element method of elastic materials, Mechanics Research Communications, 31(3) (2004) 321-330.
[40]. H. Wang, Q.-H. Qin, Numerical implementation of local effects due to two-dimensional discontinuous loads using special elements based on boundary integrals, Engineering Analysis with Boundary Elements, 36(12) (2012) 1733-1745.
[41]. Q.H. Qin, Formulation of hybrid Trefftz finite element method for elastoplasticity, Applied Mathematical Modelling, 29(3) (2005) 235-252.
[42]. Q.-H. Qin, Trefftz plane elements of elastoplasticity with p-extension capabilities, Journal of Mechanical Engineering, 56(1) (2005) 40-59.
[43]. Y. Cui, Q.H. Qin, Fracture analysis of mode III problems by Trefftz finite element approach, in: WCCM VI in conjunction with APCOM, 2004, pp. v1-p380.
[44]. Y.-h. Cui, Q.H. Qin, J.-S. Wang, Application of HT finite element method to multiple crack problems of Mode I, II and III, Chinese Journal of Engineering Mechanics, 23(3) (2006) 104-110.
[45]. Y. Cui, J. Wang, M. Dhanasek, Q.H. Qin, Mode III fracture analysis by Trefftz boundary element method, Acta Mechanica Sinica, 23(2) (2007) 173-181.
[46]. C. Cao, Q.H. Qin, A. Yu, Micromechanical Analysis of Heterogeneous Composites using Hybrid Trefftz FEM and Hybrid Fundamental Solution Based FEM, Journal of Mechanics, 29(4) (2013) 661-674.
[47]. C. Cao, A. Yu, Q.H. Qin, Evaluation of effective thermal conductivity of fiber-reinforced composites by boundary integral based finite element method, International Journal of Architecture, Engineering and Construction, 1(1) (2012) 14-29.
[48]. M. Dhanasekar, J. Han, Q.H. Qin, A hybrid-Trefftz element containing an elliptic hole, Finite Elements in Analysis and Design, 42(14) (2006) 1314-1323.
[49]. Q.H. Qin, X.-Q. He, Special elliptic hole elements of Trefftz FEM in stress concentration analysis, Journal of Mechanics and MEMS, 1(2) (2009) 335-348.
[50]. J. Jirousek, Q.H. Qin, Application of hybrid-Trefftz element approach to transient heat conduction analysis, Computers & Structures, 58(1) (1996) 195-201.
[51]. L. Cao, Q.H. Qin, N. Zhao, Application of DRM-Trefftz and DRM-MFS to Transient Heat Conduction Analysis, Recent Patents on Space Technology (Open access), 2 (2010) 41-50.
[52]. N. Zhao, L.-L. Cao, Q.-H. Qin, Application of Trefftz Method to Heat Conduction Problem in Functionally Graded Materials, Recent Patents on Space Technology, 1(2) (2011) 158-166.
[53]. Q.H. Qin, Hybrid Trefftz finite-element approach for plate bending on an elastic foundation, Applied Mathematical Modelling, 18(6) (1994) 334-339.
[54]. Q.H. Qin, Postbuckling analysis of thin plates by a hybrid Trefftz finite element method, Computer Methods in Applied Mechanics and Engineering, 128(1) (1995) 123-136.
[55]. Q.H. Qin, Transient plate bending analysis by hybrid Trefftz element approach, Communications in Numerical Methods in Engineering, 12(10) (1996) 609-616.
[56]. Q.H. Qin, Postbuckling analysis of thin plates on an elastic foundation by HT FE approach, Applied Mathematical Modelling, 21(9) (1997) 547-556.
[57]. F. Jin, Q.H. Qin, A variational principle and hybrid Trefftz finite element for the analysis of Reissner plates, Computers & Structures, 56(4) (1995) 697-701.
[58]. J. Jirousek, A. Wroblewski, Q.H. Qin, X. He, A family of quadrilateral hybrid-Trefftz p-elements for thick plate analysis, Computer Methods in Applied Mechanics and Engineering, 127(1) (1995) 315-344.
[59]. Q.H. Qin, Hybrid-Trefftz Finite-Element Method for Reissner Plates on an Elastic-Foundation, Computer Methods in Applied Mechanics and Engineering, 122(3-4) (1995) 379-392.

[60]. Q.H. Qin, S. Diao, Nonlinear analysis of thick plates on an elastic foundation by HT FE with p-extension capabilities, International Journal of Solids and Structures, 33(30) (1996) 4583-4604.

[61]. Q.H. Qin, Nonlinear analysis of thick plates by HT FE approach, Computers & Structures, 61(2) (1996) 271-281.

[62]. C.-Y. Lee, Q.H. Qin, H. Wang, Trefftz functions and application to 3D elasticity, Computer Assisted Mechanics and Engineering Sciences, 15 (2008) 251-263.

[63]. Q.H. Qin, Variational formulations for TFEM of piezoelectricity, International Journal of Solids and Structures, 40(23) (2003) 6335-6346.

[64]. Q.H. Qin, Solving anti-plane problems of piezoelectric materials by the Trefftz finite element approach, Computational Mechanics, 31(6) (2003) 461-468.

[65]. Q.H. Qin, Mode III fracture analysis of piezoelectric materials by Trefftz BEM, Structural Engineering and Mechanics, 20(2) (2005) 225-240.

[66]. Q.H. Qin, Fracture Analysis of Piezoelectric Materials by Boundary and Trefftz Finite Element Methods, WCCM VI in conjunction with APCOM'04, Sept. 5-10, 2004, Beijing, China, (2004).

[67]. Q.H. Qin, Trefftz Plane Element of Piezoelectric Plate with p-Extension Capabilities, IUTAM Symposium on Mechanics and Reliability of Actuating Materials, (2006) 144-153.

[68]. Q.H. Qin, K.-Y. Wang, Application of hybrid-Trefftz finite element method fractional contact problems, Computer Assisted Mechanics and Engineering Sciences, 15 (2008) 319-336.

[69]. K. Wang, Q.H. Qin, Y. Kang, J. Wang, C. Qu, A direct constraint-Trefftz FEM for analysing elastic contact problems, International Journal for Numerical Methods in Engineering, 63(12) (2005) 1694-1718.

[70]. M. Dhanasekar, K.Y. Wang, Q.H. Qin, Y.L. Kang, Contact analysis using Trefftz and interface finite elements, Computer Assisted Mechanics and Engineering Sciences, 13(3) (2006) 457-471.

[71]. H. Wang, Q.H. Qin, Hybrid FEM with fundamental solutions as trial functions for heat conduction simulation, Acta Mechanica Solida Sinica, 22(5) (2009) 487-498.

[72]. C. Cao, Q.-H. Qin, Hybrid fundamental solution based finite element method: theory and applications, Advances in Mathematical Physics, 2015 (2015).

[73]. Q.H. Qin, Fundamental Solution Based Finite Element Method, J Appl Mech Eng, 2 (2013) e118.

[74]. Z.-J. Fu, W. Chen, Q.H. Qin, Hybrid Finite Element Method Based on Novel General Solutions for Helmholtz-Type Problems, Computers Materials and Continua, 21(3) (2011) 187.

[75]. Y.-T. Gao, H. Wang, Q.-H. Qin, Orthotropic Seepage Analysis using Hybrid Finite Element Method, Journal of Advanced Mechanical Engineering, 2(1) (2015) 1-13.

[76]. H. Wang, Q.H. Qin, Fundamental solution-based hybrid finite element analysis for non-linear minimal surface problems, Recent Developments in Boundary Element Methods: A Volume to Honour Professor John T. Katsikadelis, 309 (2010).

[77]. H. Wang, Q.-H. Qin, Fundamental-solution-based hybrid FEM for plane elasticity with special elements, Computational Mechanics, 48(5) (2011) 515-528.

[78]. H. Wang, Q.H. Qin, W. Yao, Improving accuracy of opening-mode stress intensity factor in two-dimensional media using fundamental solution based finite element model, Australian Journal of Mechanical Engineering, 10(1) (2012) 41-51.

[79]. Q.H. Qin, H. Wang, Special Elements for Composites Containing Hexagonal and Circular Fibers, International Journal of Computational Methods, 12(04) (2015) 1540012.

[80]. H. Wang, Q.H. Qin, Special fiber elements for thermal analysis of fiber-reinforced composites, Engineering Computations, 28(8) (2011) 1079-1097.

[81]. H. Wang, Q.H. Qin, A fundamental solution based FE model for thermal analysis of nanocomposites, in: Boundary elements and other mesh Reduction methods XXXIII', 33rd International Conference on Boundary Elements and other Mesh Reduction Methods, ed. CA Brebbia and V. Popov, WIT Press, UK, 2011, pp. 191-202.

[82]. H. Wang, Q.H. Qin, Implementation of fundamental-solution based hybrid finite element model for elastic circular inclusions, in: Proceedings of the Asia-Pacific Congress for Computational Mechanics, 11th-14th Dec, 2013.

[83]. C. Cao, Q.H. Qin, A. Yu, Modelling of Anisotropic Composites by Newly Developed HFS-FEM, in: Proceedings of the 23rd International Congress of Theoretical and Applied Mechanics, Yilong Bai , Jianxiang Wang , Daining Fang (eds), SM08-016, August 19 - 24 , 2012, Beijing, China, The International Union of Theoretical and Applied Mechanics (IUTAM), 2012.

[84]. C. Cao, Q.H. Qin, A. Yu, Hybrid fundamental-solution-based FEM for piezoelectric materials, Computational Mechanics, 50(4) (2012) 397-412.

[85]. C. Cao, A. Yu, Q.-H. Qin, A new hybrid finite element approach for plane piezoelectricity with defects, Acta Mechanica, 224(1) (2013) 41-61.

[86]. H. Wang, Q.H. Qin, Fracture analysis in plane piezoelectric media using hybrid finite element model, in: International Conference of fracture, 16-21 June, 2013, Beijing, China, 2013.

[87]. C. Cao, Q.-H. Qin, A. Yu, A new hybrid finite element approach for three-dimensional elastic problems, Archives of Mechanics, 64(3) (2012) 261-292.

[88]. L.-L. Cao, Q.-H. Qin, N. Zhao, Hybrid graded element model for transient heat conduction in functionally graded materials, Acta Mechanica Sinica, 28(1) (2012) 128-139.

[89]. L. Cao, H. Wang, Q.-H. Qin, Fundamental solution based graded element model for steady-state heat transfer in FGM, Acta Mechanica Solida Sinica, 25(4) (2012) 377-392.

[90]. H. Wang, Q.-H. Qin, Boundary integral based graded element for elastic analysis of 2D functionally graded plates, European Journal of Mechanics-A/Solids, 33 (2012) 12-23.

[91]. H. Wang, Q.H. Qin, FE approach with Green's function as internal trial function for simulating bioheat transfer in the human eye, Archives of Mechanics, 62(6) (2010) 493-510.

[92]. H. Wang, Q.H. Qin, Computational bioheat modeling in human eye with local blood perfusion effect, Human Eye Imaging and Modeling, (2012).

[93]. H. Wang, Q.-H. Qin, A fundamental solution-based finite element model for analyzing multi-layer skin burn injury, Journal of Mechanics in Medicine and Biology, 12(05) (2012) 1250027.

[94]. Z.-W. Zhang, H. Wang, Q.-H. Qin, Transient bioheat simulation of the laser-tissue interaction in human skin using hybrid finite element formulation, Molecular & Cellular Biomechanics, 9(1) (2012) 31-53.

[95]. Z.W. Zhang, H. Wang, Q.H. Qin, Analysis of transient bioheat transfer in the human eye using hybrid finite element model, in: Applied Mechanics and Materials, Trans Tech Publ, 2014, pp. 356-361.

[96]. J. Tao, Q.H. Qin, L. Cao, A Combination of Laplace Transform and Meshless Method for Analysing Thermal Behaviour of Skin Tissues, Universal Journal of Mechanical Engineering, 1(2) (2013) 32-42.

[97]. Z.W. Zhang, H. Wang, Q.H. Qin, Method of fundamental solutions for nonlinear skin bioheat model, Journal of Mechanics in Medicine and Biology, 14(4) (2014) 1450060.

[98]. C. Cao, Q.-H. Qin, A. Yu, A novel boundary-integral based finite element method for 2D and 3D thermo-elasticity problems, Journal of Thermal Stresses, 35(10) (2012) 849-876.

[99]. Q.H. Qin, H. Wang, Special circular hole elements for thermal analysis in cellular solids with multiple circular holes, International Journal of Computational Methods, 10(04) (2013) 1350008.

[100]. H. Wang, Q.-H. Qin, A new special element for stress concentration analysis of a plate with elliptical holes, Acta Mechanica, 223(6) (2012) 1323-1340.

[101]. Q.H. Qin, H. Wang, Fundamental solution based FEM for nonlinear thermal radiation problem, in: 12th International Conference on Boundary Element and Meshless Techniques (BeTeq 2011), ed. EL Albuquerque, MH Aliabadi, EC Ltd, Eastleigh, UK, 2011, pp. 113-118.

[102]. C. Cao, A. Yu, Q.-H. Qin, A novel hybrid finite element model for modeling anisotropic composites, Finite Elements in Analysis and Design, 64 (2013) 36-47.

[103]. C. Cao, A. Yu, Q.H. Qin, Mesh reduction strategy: Special element for modelling anisotropic materials with defects, Boundary Elements and Other Mesh Reduction Methods XXXVI, 56 (2013) 61.
[104]. H. Wang, Q.-H. Qin, Fundamental-solution-based finite element model for plane orthotropic elastic bodies, European Journal of Mechanics-A/Solids, 29(5) (2010) 801-809.
[105]. C. Talischi, G.H. Paulino, A. Pereira, I.F. Menezes, PolyMesher: a general-purpose mesh generator for polygonal elements written in Matlab, Structural and Multidisciplinary Optimization, 45(3) (2012) 309-328.
[106]. Q. Du, V. Faber, M. Gunzburger, Centroidal Voronoi tessellations: Applications and algorithms, SIAM review, 41(4) (1999) 637-676.
[107]. C. Talischi, G.H. Paulino, A. Pereira, I.F. Menezes, PolyTop: a Matlab implementation of a general topology optimization framework using unstructured polygonal finite element meshes, Structural and Multidisciplinary Optimization, 45(3) (2012) 329-357.
[108]. G. Fairweather, A. Karageorghis, The method of fundamental solutions for elliptic boundary value problems, Advances in Computational Mathematics, 9(1-2) (1998) 69.
[109]. T.H. Pian, C.-C. Wu, Hybrid and incompatible finite element methods, CRC Press, 2005.